DOI: 10.5604/01.3001.0013.7622

Journal of Achievements in Materials and Manufacturing Engineering

International Scientific Journal published monthly by the World Academy of Materials and Manufacturing Engineering

Laser cladding of Co-based metallic powder at cryogenic conditions

A. Lisiecki [a,*], D. Ślizak [b], A. Kukofka [a,b]

[a] Department of Welding Engineering, Faculty of Mechanical Engineering, Silesian University of Technology, ul. Konarskiego 18a, 44-100 Gliwice, Poland

[b] PROGRESJA, ul. 1 Maja 35, 41-940 Piekary Śląskie, Poland

* Corresponding e-mail address: aleksander.lisiecki@polsl.pl

ABSTRACT

Purpose: of this paper was demonstration a novel technique of laser cladding by experimentally composed Co-based metallic powder and forced cooling of the substrate by liquid nitrogen under cryogenic conditions, at the temperature -190°C, for producing clad layers with enhanced microstructure characteristic and properties.

Design/methodology/approach: Technological tests of laser cladding were conducted by means of a high power fibre laser HPFL with maximum output power 3.0 kW, and six-axis robot. The experimental Co-based powder was composed for providing high abrasive wear resistance, high resistance for impact load, and also for corrosion resistance at elevated temperature. The unique and novel technique of forced cooling of the substrate was provided by immersing the specimens in the liquid nitrogen bath. The three coaxial nozzle head was designed and custom made to provide precise deposition of the powder delivered into the laser beam irradiation region. The scope of the study included tests of conventional laser cladding at free cooling in ambient air in a wide range of processing parameters, and also trials of laser cladding under cryogenic conditions. The test clad layers produced by conventional laser cladding and by the novel technique of laser powder deposition under cryogenic conditions were investigated and compared.

Findings: The obtained results indicate that the novel technique of forced cooling the substrate by liquid nitrogen bath provides lower penetration depth, as well as low dilution of the clad, and also provides higher hardness of the clads. Additionally, it is possible shaping the geometry of the individual bead, providing high reinforcement and low width.

Research limitations/implications: The presented results are based just on preliminary test of the novel technique of laser cladding under cryogenic conditions. Therefore, further study and detailed analyse of the influence of the cooling rate on the quality, microstructure, and properties of the deposited coatings are required.

Practical implications: The study is focused on practical application of the novel technique for manufacturing of wear resistance coatings characterised with enhanced performance compared to conventional range of application of the laser cladding.

Originality/value: Novel technique of laser cladding at forced cooling under cryogenic conditions was demonstrated. The powder used for cladding trials was experimentally composed (not commercially available). The experimental stand custom made was used with custom made powder feeding rate, and also with custom made coaxial nozzle head.

Keywords: Laser cladding, Cobalt-based powder, Cryogenic conditions, Forced cooling

Reference to this paper should be given in the following way:
A. Lisiecki, D. Ślizak, A. Kukofka, Laser cladding of Co-based metallic powder at cryogenic conditions, Journal of Achievements in Materials and Manufacturing Engineering 95/1 (2019) 20-31.

MANUFACTURING AND PROCESSING

1. Introduction

Laser surface cladding (LSC) is very advantageous method for manufacturing of metallic and composite coatings [1-6]. One area of application for laser cladding is manufacturing of wear resistant or corrosion resistant coatings [7-12]. The advantage of laser cladding over other methods of cladding such as arc, plasma or flame cladding is the high power density, localized heating, high processing speed, and limited thermal influence on the substrate. Therefore, laser cladding provides low dilution and fine-grained microstructure in general [13]. However, constant pursuit for improving properties and durability of the working surfaces of components and tools forces the search for new and improved coatings materials, as well as new or improves methods of their manufacturing [14-24].

In turn, among the alloys providing high wear resistance, and corrosion resistance even at elevated temperature, the Co-based alloys play significant role [2,3]. The most common is the group of Co alloys containing also high amount of chromium and usually also tungsten and molybdenum, known under a trademark "stellite". Depending of the composition and proportions between the components the properties of Co-based alloys may be shaped and customized in a wide range. Therefore, this group of alloys are widely used in the industry. Excellent properties of the "stellite" type coatings are the result of high corrosion resistance in liquid and gaseous environments of solid solution of cobalt, and also presence of fine dispersive carbides, which provide excellent tribological properties, especially high abrasive wear resistance. Different methods of stellite type coatings were widely investigated and described in the literature. Similarly, the properties and microstructure study of such coatings are thoroughly described in the literature [2,3,25].

For example, A. Zieliński et al. have investigated properties of two types of Co-based coatings on exhaust valves of marine diesel engines produced by laser cladding [2]. They found that the clad layers are characterized by high quality, and small grain directional dendrites of subeutectic structure. J. Xiong et al. have investigated the microstructure evolution and failure behaviour of Stellite 6 coating produced by TIG cladding on steel substrate after long-time service [26]. They discovered diffusion of Fe from the substrate into the coating affected its properties after long-time operation. They also provide wide and comprehensive review of the literature and state of the art in the field of stellite type coating technology. For example, Ferozhkhanet et al. investigated the process of plasma transferred arc coating of Stellite 6 alloy on steel 309L [27]. Mirshekariet et al. [28], and also Molleda et al. [29] have investigated TIG cladding of stellite coating on steel substrate. They both reported some inconvenience of the coating due to crack occurrence after long-time service at high temperature and high pressure. In such long-term studies of structures behaviour (coatings or welded joints) the numerical analysis is a useful tool, [30-34]. Another recent example of research in the field of Co-based coatings is the study of Z. Wang et al., who have investigated microstructure and properties of laser metal deposited H465/Stellite-6 laminated material [35]. They found that such laminated material shows lower tendency for cracking compared to single K465 superalloy produce under LMD process.

On the other hand the technology of cryogenic treatment (CT) is widely used at the manufacturing process of different metal components such cutting tools, measuring devices or precise components for enhancing the mechanical properties [36]. The cryogenic treatment can be divided into three main groups such cold treatment, shallow cryogenic treatment (SCT), and deep cryogenic treatment (DCT) depending on the temperature range [36]. In the case of cold treatment the temperature range is between 193 and 273 K, while in a case of shallow cryogenic treatment the temperature range is 113-193 K, and in deep cryogenic treatment the range is 77-113 K [36]. It is widely reported that the cryogenic treatment of metals and alloys can enhance mechanical properties and also wear characteristics.

An original technique combining laser surface treatment with cryogenic treatment was proposed and demonstrated by A. Zieliński and his research team [37-39]. They investigated laser surface melting of non-ferrous alloys such titanium, aluminium, and cooper alloys under cryogenic conditions provided by immersing the substrate in liquid nitrogen. In such a way they provided ultrafast quenching of melted layers in presence of nitrogen.

In this study an attempt has been made to conduct preliminary tests of laser cladding by Co-based powder with simultaneous forced cooling the substrate by liquid nitrogen, providing cryogenic conditions of laser cladding process. The level of complexity of such a process is significantly higher than in a case of surface melting. Such proposed novel technique combines laser cladding, simultaneous laser alloying by the evaporated nitrogen as active gas, and the atomic N as an alloying element, additionally conducted under cryogenic conditions.

Therefore, the novel process was considered as hybrid laser surface processing at cryogenic conditions.

2. Materials and the methodology

In order to minimize the influence of the substrate material on the process of laser cladding and also the composition and properties of the test clad layers, non-alloy structural steel (S235) was chosen for the study. The chemical composition of the steel substrate is given in Table 1, while the microstructure is shown in Figure 1. The specimens of the substrate were laser cut into coupons 100x100 mm from a flat plate with the thickness 5.0 mm. The specimens were sandblasted and cleaned by alcohol prior to the laser cladding trials.

Table 1.
Chemical composition of the non-alloy structural steel S235 (according to EN 10025-2:2004)

C	Mn	Si	P	S	Fe
0.22	1.6	0.05	0.05	0.05	Bal.

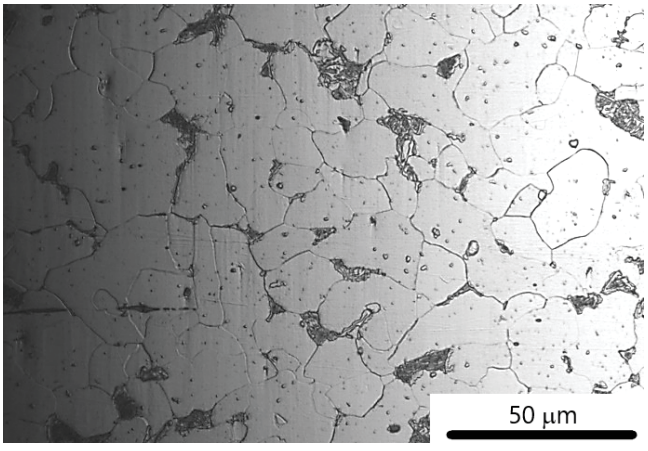

Fig. 1. Microstructure of the substrate, steel S235

The composition of the experimental metallic powder was designed in such a way to provide high abrasive wear resistance, and simultaneously high impact load resistance, and corrosion resistance at elevated temperature. The powder was based on cobalt with addition mainly of chromium and tungsten. Therefore, the experimental powder was designed as Co-based powder. Detailed chemical composition of the powder is given in Table 2. The particles size distribution of the cobalt-based metal powder was 60-160 µm.

Table 2.
Composition of Co-based experimental powder (wt.%)

Cr	W	C	Si	Ni	Fe	Co
26.5-27.0	7.5-8.0	1.3-1.4	1.15	0.9-1.0	0.95-1.1	Bal.

The tests of laser cladding were conducted by means of an experimental stand equipped with a six-axis robot Panasonic GII TL-190, high power fibre laser (HPFL) IPG YLS-3000, a custom made powder feeding system consisted of rotary feeder, head with three coaxial nozzles, and also with a bath of liquid nitrogen for forced cooling of the substrate during cladding. The bottom and side walls of the bath were thermally isolated by polyurethane foam. The experimental stand is shown in Figure 2.

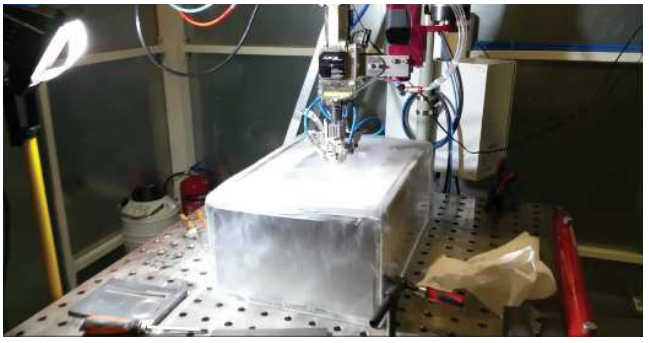

Fig. 2. A view of the experimental stand for laser cladding tests with a bath of liquid nitrogen

The laser was characterized by maximum output power of 3.0 kW, circular laser beam with the spot diameter 300 µm and a single mode energy distribution across the spot. In order to provide wider stringer beads the laser beam was defused by lifting the laser head 30 mm over the top surface of the substrate steel specimen. As a result of defocusing, the area irradiated by the laser beam on the top surface was 1.3 mm in diameter.

The single stringer beads were produced at different energy input under free cooling and forced cooling, when the specimen was immerged in the liquid nitrogen bath. The length of the beads was 40.0 mm, while the side shift 10.0 mm. The powder was delivered in argon as the carrier gas, and the three powder streams from the individual nozzles were focused on the surface of the melt pool. The powder feeding rate was maintained constant at 6.0 g/min. The laser beam power was ranged from 250 W to 1000 W, while the processing speed was ranged from 250 mm/min to 1000 mm/min.

The laser beam was transmitted via a cylindrical nozzle in argon atmosphere, at the flow rate 20.0 l/min. The nozzle with a diameter of 10.0 mm was set perpendicular to the specimen surface. The argon flow was also used as shielding gas.

The free cooling conditions of the clad layers during laser cladding were provided by a natural cooling of the specimen in the ambient air. On the other hand, the cryogenic conditions were provide by partial immerging the steel specimen substrate in the liquid nitrogen bath with the temperature approx. -190°C, Figure 3. Due to intensive evaporation of the nitrogen from the liquid state, the gaseous nitrogen was present in the cladding region also, as can be seen in Figure 2. The gaseous nitrogen as active gas can also act as the alloying medium. Therefore, under such conditions the laser cladding can be considered as a hybrid process combining the processes of conventional laser cladding by powder deposition and laser gas alloying by nitrogen (in specific laser gas nitriding) enrichment of the cladded layer, additionally carried out under cryogenic forced cooling. Detailed processing parameters, as well as other relevant technological conditions are given in Tables 3 and 4. The test clad layers were examined by visual inspection first. The observations and comments regarding the quality assessment of the test layers are also given in the Tables 3 and 4. After the visual inspection the clad layers were cut perpendicularly and samples for further analysis were prepared. The samples were mounted in epoxy cold mounting resin, next grinded by water papers with grit 120 to 2000, and polished by 2 µm diamond suspension. The microstructure was disclosed by HNO_3 +3HCL reagent. Macrostructure and microstructure of the surface layers was analysed by optical microscopy (OM), by means of OLYMPUS SZX9 and NIKON Eclipse MA100. Microhardness distribution was determined on the cross-section of the test clad layers by Vickers test at the load 1000 g and the dwell time 10 s, by means of hardness tester WILSON WOLPERT 401 MVD. The measurements were taken from the under top surface (face of the clad) region, via the clad (fusion zone), next heat affected zone, to the base metal of the substrate. The distance between the subsequent points was 200 µm. The measuring line was set vertically on the symmetry axis of the clad layer. Based on the single clad layer geometry determined on the macrographs, the influence of the process parameters and cooling conditions on the shape and quality of the clads was determined.

a) b)

Fig. 3. A view of the (a) fibre laser IPG YLS – 3000 and (b) a rotary powder feeder

Table 3.
Parameters of laser cladding by the experimental Co-based metal powder at free cooling in the ambient air (conventional laser cladding), and quality assessment of test clad layers

No.	Surface layer mark	Scanning speed, mm/min	Laser power, W	Energy input, J/mm	Quality assessment
1	NS1	250	250	60	IF
2	NS2	250	500	120	HQ
3	NS3	250	750	180	HQ
4	NS4	250	1000	240	SP
5	NS5	500	250	30	IF
6	NS6	500	500	60	UB
7	NS7	500	750	90	SP
8	NS8	500	1000	120	SP
9	NS9	750	250	20	IF
10	NS10	750	500	40	UB
11	NS11	750	750	60	HQ
12	NS12	750	1000	80	V
13	NS13	1000	250	15	IF
14	NS14	1000	500	30	HQ
15	NS15	1000	750	45	UB, SP
16	NS16	1000	1000	60	SP

Other parameters and conditions of deposition; beam spot diameter: 300.0 μm, focal spot position: + 30 mm, diameter of shielding nozzle: 10.0 mm, shielding and feeding gas: high purity Ar (99.999%), shielding gas flow rate: 20.0 l/min, powder feeding rate: 6.0 g/min, powder feeding gas flow: 8.0 l/min. Remarks: UB – uneven bead, SP – single pore, IF – incomplete fusion, V – voids, HQ – high quality

Table 4.
Parameters of laser cladding by the experimental Co-based metal powder at forced cooling by liquid nitrogen (hybrid cryogenic method), and quality assessment of test clad layers

No.	Surface layer mark	Scanning speed, mm/min	Laser power, W	Energy input, J/mm	Quality assessment
1	NW1	250	250	60	LF
2	NW2	250	500	120	LF
3	NW3	250	750	180	LF
4	NW4	250	1000	240	IF, OL
5	NW5	500	250	30	LF
6	NW6	500	500	60	IF
7	NW7	500	750	90	IF, OL
8	NW8	500	1000	120	IF, ER
9	NW9	750	250	20	LF
10	NW10	750	500	40	UB
11	NW11	750	750	60	UB
12	NW12	750	1000	80	UB
13	NW13	1000	250	15	IF
14	NW14	1000	500	30	UB
15	NW15	1000	750	45	SP
16	NW16	1000	1000	60	SP

Other parameters and conditions of deposition; beam spot diameter: 300.0 μm, focal spot position: + 30 mm, diameter of shielding nozzle: 10.0 mm, shielding and feeding gas: high purity Ar (99.999%), shielding gas flow rate: 20.0 l/min, powder feeding rate: 6.0 g/min, powder feeding gas flow: 8.0 l/min. Remarks: LF – Lack of fusion, OL – overlap, UB – uneven bead, ER – excessive reinforcement, SP – single pore, IF – incomplete fusion

Regarding the geometry of the test clad layers, a width of the clad, a width of the heat affected zone, and also the penetration depth were determined for the representative clad layers. The obtained results of the study of laser cladding at free cooling and forced cryogenic cooling by liquid nitrogen are presented in Figures from 4 to 13 and Tables from 3 to 6.

Table 5.
Hardness HV1 distribution on cross-section of the test clad layers produced by laser cladding of Co-based powder at free cooling, Table 3

Distance from the top surface mm	Clad No.		
	NS4	NS11	NS14
0.15	**348**	**278**	**307**
0.25	370	295	328
0.35	353	309	308
0.55	344	319	236
0.75	343	286	207
0.95	336	219	179
1.15	335	169	145
1.35	292	143	-
1.55	265	-	-
1.75	218	-	-
1.95	204	-	-
2.15	182	-	-
2.35	151	-	-

Table 6.
Hardness HV1 distribution on cross-section of the test clad layers produced by laser cladding of Co-based powder at forced cooling in cryogenic conditions, Table 4

Distance from the top surface mm	Clad No.		
	NS4	NS11	NS14
0.15	**603**	**541**	**465**
0.25	602	604	496
0.35	535	599	478
0.55	566	574	476
0.75	633	572	481
0.95	446	566	468
1.15	232	400	239
1.35	155	263	144
1.55	143	164	-
1.75	-	140	-

3. Results and discussion

The task of the conducted tests was the comparative analysis of laser cladding of Co-based metal powder at conventional conditions and free cooing of the substrate in ambient air, and also the proposed novel technique of laser cladding under forced cooling in cryogenic conditions provided by liquid nitrogen bath at the temperature -190°C.

The visual inspection of the test clad layers produced both under conventional laser cladding conditions at free cooling, and also under cryogenic conditions showed that the face surfaces (top surface of the stringer beads) of the clads have high roughness, and also the width and reinforcement are strongly influenced by the process parameters in the investigated range of parameters, Figure 3.

The first cursory observations of the test clads showed that the stringer beads produced in the range of the low energy inputs and at cryogenic conditions provided by the liquid nitrogen bath may show incomplete penetration or even partial lack of fusion.

The suspicions have been confirmed by observations of the cross-sections of the tests clads. As can be seen in Figures 4 to 6, the energy input of laser cladding has significant influence on the geometry of the beads, thus also on the penetration depth and dilution. However, in the case of test clads produced under cryogenic conditions, additionally at the lowest laser output power of 250 W, lack of fusion was confirmed. Therefore, for further analysis just clad layers with a complete penetration of the substrate were chosen.

A comparison of the shape and geometrical features of the clad layers produced at different cooling conditions indicates that the clads produced at forced cooling at cryogenic conditions are characterized by the highest reinforcement, and simultaneously the lowest width, as can be seen on macrographs and the graphs presented in Figures 7 and 8. This phenomenon is a result of limited penetration depth due to supercooled steel substrate. As a result, the dilution is very low, and the powder delivered into the region of laser beam interaction is melted and deposited on the substrate. On the other hand, the surface tension acts such that the molten powder tends to take a spherical shape, with limited ability to wet the substrate. Therefore, the clad layers produced at cryogenic conditions are high, and narrow, if compared to the clads produced by conventional technique of laser cladding, Figures 4 to 8. The obtained results indicate that the technique of forced cooling of the substrate during laser cladding can be considered as an effective way for shaping the geometry of the clads and minimizing the dilution of the substrate material. It is especially of importance during cladding thin

coatings with completely different chemical or/and phase composition than the substrate.

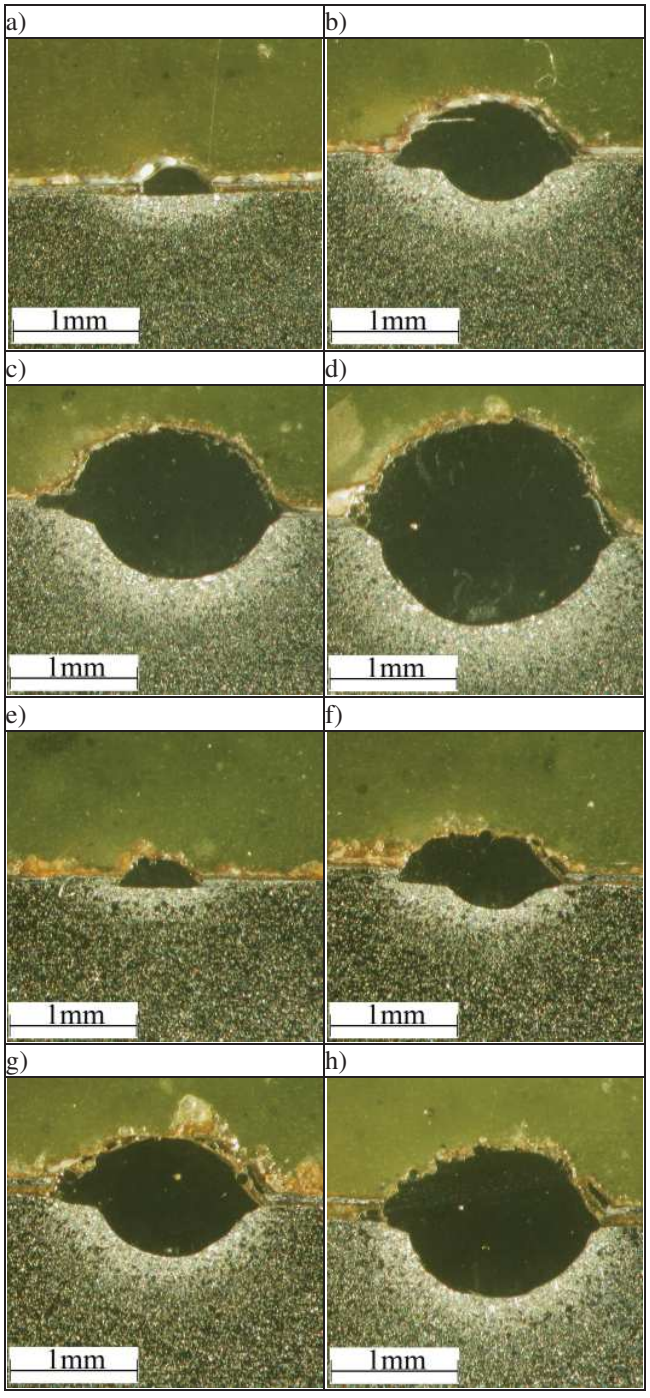

Fig. 4. Macrostructure of test clad layers produced by laser cladding of Co-based metal powder at free cooling in ambient air (Tab. 3); a) NS1, b) NS2, c) NS3, d) NS4, e) NS5, f) NS6, g) NS7, h) NS8

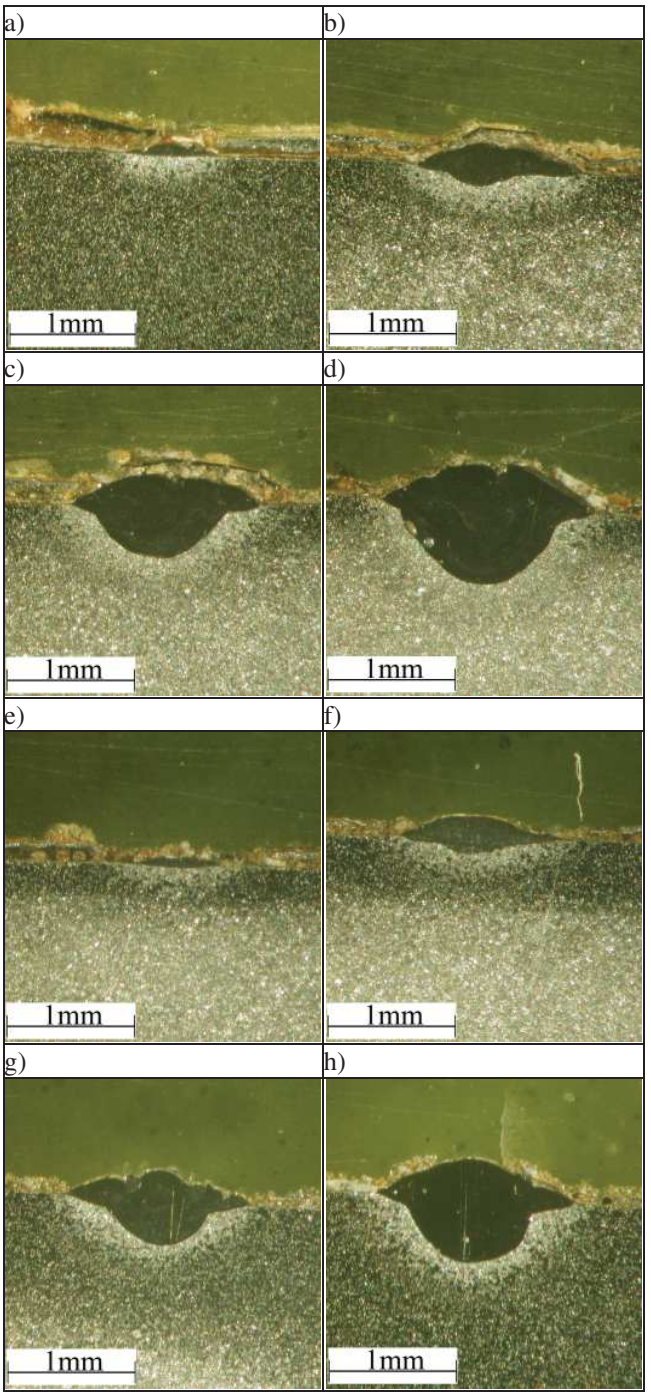

Fig. 5. Macrostructure of test clad layers produced by laser cladding of Co-based metal powder at free cooling in ambient air (Tab. 3); a) NS9, b) NS10, c) NS11, d) NS12, e) NS13, f) NS14, g) NS15, h) NS16

Comparative assessment of the quality of test clad layers, beside the evident differences in the geometry and

dilution, showed higher tendency for porosity and voids in a case of clads produced at forced cooling under cryogenic conditions, as can be seen in Figures 6e,f, and in Table 4. This phenomenon may be explained also by the thermal conditions related with forced and therefore accelerated cooling of the melt pool. Under such conditions the time of being at the liquid state is shorter. Therefore, the conditions for degassing of the melt pool are not favourable.

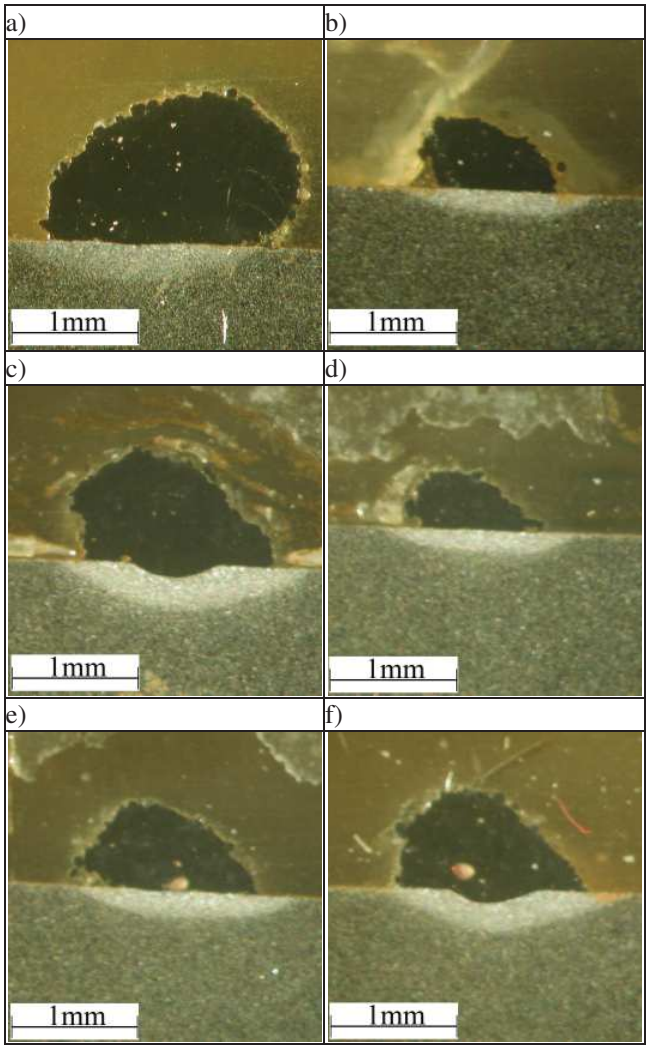

Fig. 6. Macrostructure of test clad layers produced by laser cladding of Co-based metal powder at forced cooling in cryogenic conditions (Tab. 4); a) NW8, b) NW10, c) NW12, d) NW14, e) NW15, f) NW16

The Vickers HV1 hardness measurement conducted on the cross-section of the test clad layers revealed distinct difference between the maximum values obtained for the clads produced by conventional technique of laser cladding and the clads produced by the novel technique comprises of forced cooling of the substrate by liquid nitrogen bath. As can be seen in Figure 10 and in Table 5 the maximum values of HV1 hardness for the clads produced at forced cooling are ranged from 450 HV1 to even 640 HV1, while the maximum values of hardness for the clads produced by conventional laser cladding reaches maximum at 370 HV1, Figure 10. The total range of the hardness for the clads produced by conventional laser cladding is from 260 HV1 to 370 HV1. Such huge difference in the hardness is directly related with the degree of dilution. Although, the dilution for individual clad layers has not been parameterised, it is clear that the dilution for the clads produced at free cooling is approx. 25 to even over 50% (with expectation of the clad NS1 with lowest dilution), as can be seen in Figures 4 and 5. In such a case the non-alloyed steel substrate comes to the clad surface.

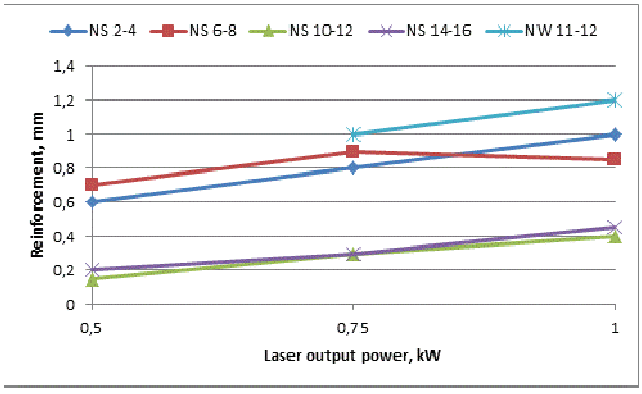

Fig. 7. Influence of the process parameters and cooling condition on the penetration depth of the test clad layers produced by laser cladding of Co-based metal (Tabs. 3, 4)

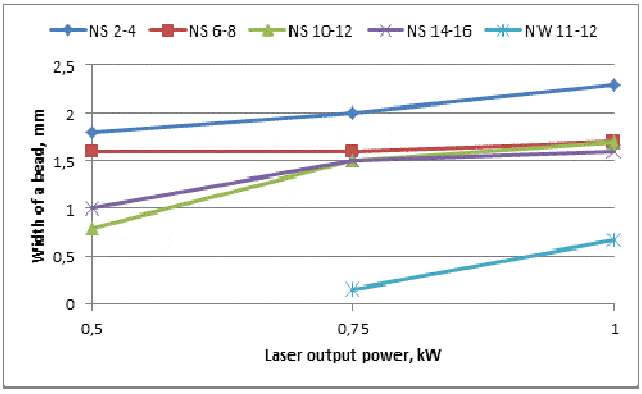

Fig. 8. Influence of the process parameters and cooling condition on the width of the test clad layers produced by laser cladding of Co-based metal (Tabs. 3, 4)

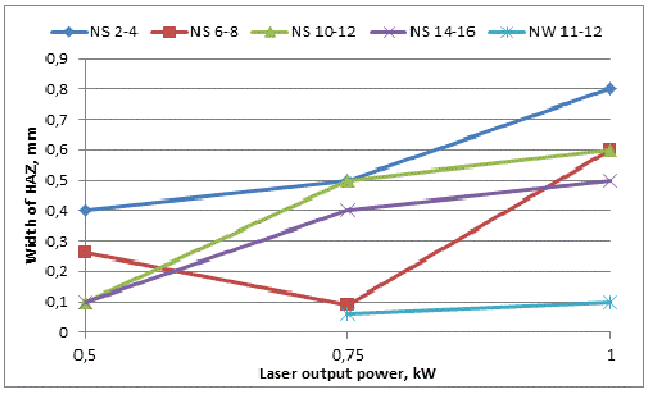

Fig. 9. Influence of the process parameters and cooling condition on the width of HAZ of the test clad layers produced by laser cladding of Co-based metal (Tabs. 3, 4)

a)

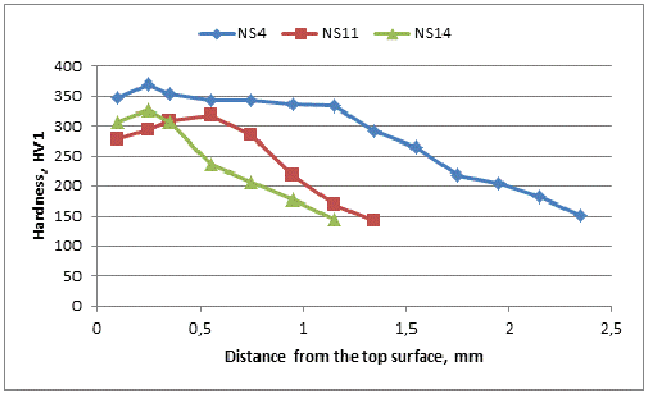

b)

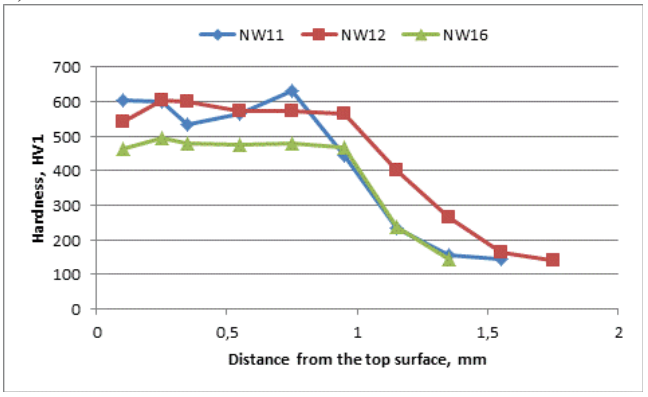

Fig. 10. Hardness distribution on cross-section of the chosen clad layers produced by laser cladding of Co-based metal powder; a) at free cooling in ambient air (Tab. 3), and b) at forced cooling in cryogenic conditions (Tab. 4)

The highest dilution, the higher share of the substrate, resulted in deterioration of the composition and properties of the clad. Therefore, it is advantageous to provide the dilution as minimum as possible.

Comparison of microstructure of clad layers produced laser deposition of Co-based powder at free cooling and forced cooling under cryogenic conditions is presented in Figures 11 and 12. The microstructure of the clad layers consisted of typical primary dendrites formed of solid solution fcc γ (Co) and interdendritic eutectic mainly γ-Co with precipitations of fine carbides M_7C_3, as can be Figures 11a and 12a.

a)

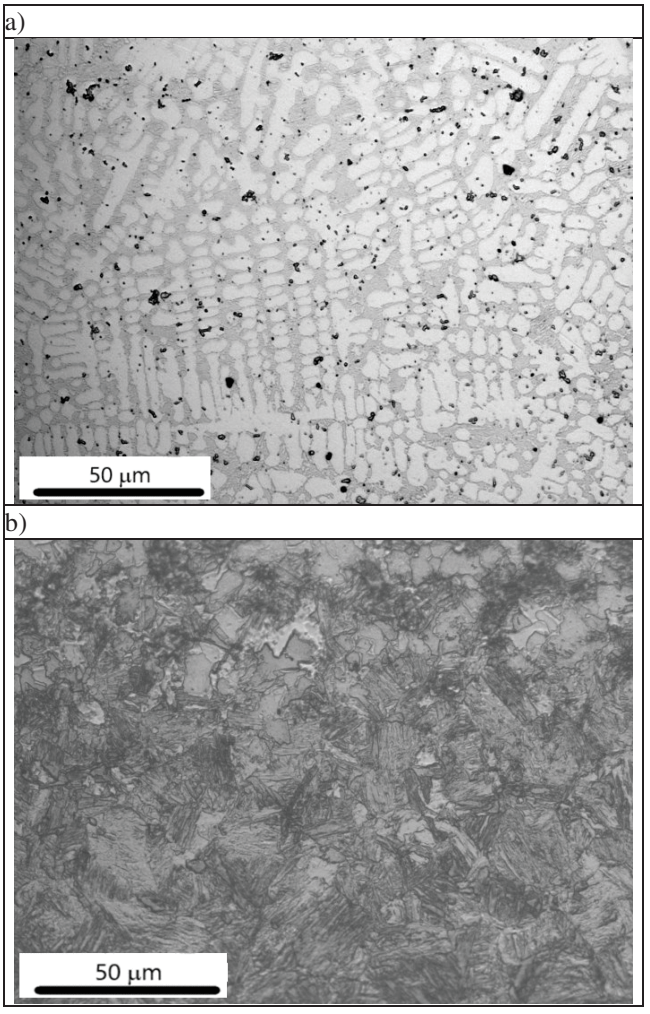

Fig. 11. Microstructure of test clad layer NS4 produced by laser cladding of Co-based metal powder at free cooling in ambient air (energy input 240 J/mm, Tab. 3), magnification 500X; a) region of clad layer, b) region of HAZ

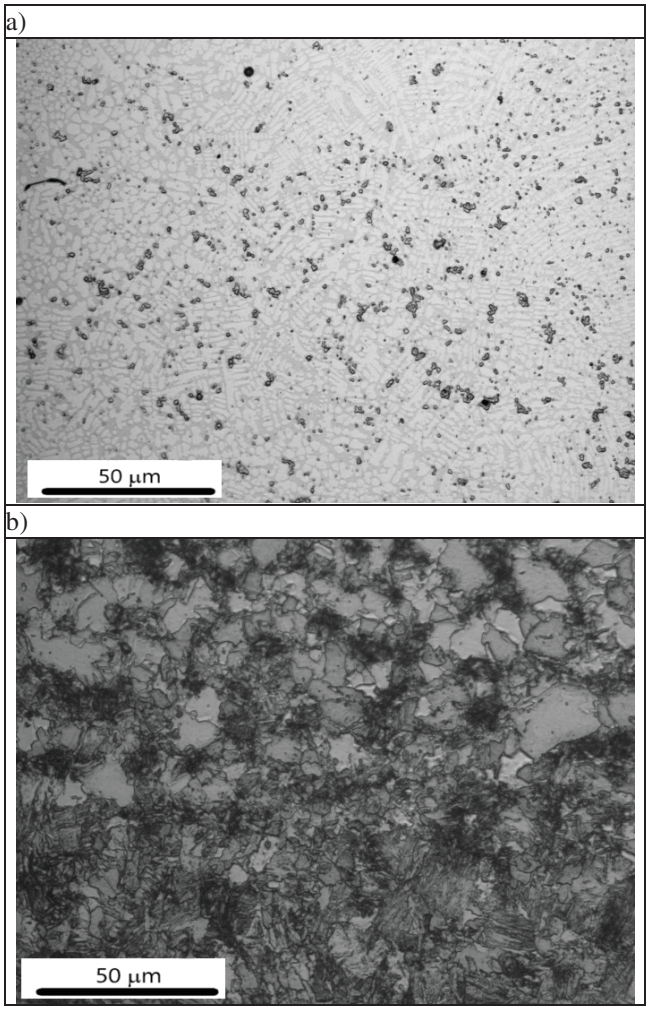

Fig. 12. Microstructure of test clad layer NW12 produced by laser cladding of Co-based metal powder at forced cooling in cryogenic conditions (energy input 80 J/mm, Tab. 4), magnification 500X; a) region of clad layer, b) region of HAZ

As can be seen many precipitates appear in the interdendritic areas. Additionally, carbides such $M_{23}C_6$, M_6C can be formed in the deposit of the experimental powder, where regarding the chemical composition the M component may be W, Cr, Co, Ni, Fe or Si (Tabs. 1 and 2). The presence of intermetallic phases such Co_3W is also possible. Moreover, due to the dilution of the steel substrate, the deposit is enriched with Fe, especially in a case of high degree of dilution. Beside the phase composition of the clad layers the size of the primary dendrites is influenced by the energy input, and conditions of cooling. As can be seen in Figures 11a and 12a the primary dendrites of the clad produced at heat input 80 J/mm and also under cryogenic conditions are very fine. The average size of the dendrites is approximately ten times smaller than the size of dendrites observed in Figure 11a. It is worth noting that the magnifications of the microstructure presented in Figures 11 and 12 are the same. Therefore, it can be concluded that the low heat input and forced cooling under cryogenic conditions lead to microstructure refinement. Regarding the heat affected zone it is also affected by the energy input of laser cladding, as well as the conditions of cooling. The microstructure of the HAZ adjacent to the clad produced at cryogenic conditions is narrower and fine-grained, compared to the HAZ of the clad produced at fee cooling, Figures 11 and 12.

4. Conclusions

The novel technique of laser cladding of Co-based powder under cryogenic conditions was successfully demonstrated. Based on the obtained results it can be concluded that the decreasing of energy input is advantageous in regard to the microstructure, and dilution. Additionally, the applied technique of supercoiling the steel substrate and forced cooling the deposited clad layer is beneficial for the microstructure refinement and geometry of the individual bead, providing limited dilution, and high reinforcement of the single bead. However, further comprehensive study on the influence of forced cooling in wider range of processing parameters on the results of laser cladding, quality, and properties of the coatings are necessary.

Acknowledgements

The study was supported by the National Centre for Research and Development, Poland, under the project POIR.01.01.01-00-0278/15-007-02, financed by EU funds.

The authors would also like to thank all those who assisted in the preparation of samples and the conducting of measurements.

References

[1] L.A. Dobrzański, A.D. Dobrzańska-Danikiewicz, T. Tański, E. Jonda, A. Drygała, M. Bonek, Laser surface treatment in manufacturing, HandBook of Manufacturing Engineering and Technology, 2015, 2677-2717.

[2] A. Zieliński, H. Smoleńska, W. Serbiński, W. Kończewicz, Characterization of the Co-base layers obtained by laser cladding technique, Journal of Materials Processing Technology 164-165 (2005) 958-963, DOI: https://doi.org/10.1016/j.jmatprotec.2005.02.093.
[3] D. Janicki, J. Górka, A. Czupryński, W. Kwaśny, M. Żuk, Diode laser cladding of Co-based composite coatings reinforced by spherical WC particles, Proceedings of SPIE 10159 (2016) 101590N, DOI: https://doi.org/10.1117/12.2261675.
[4] G. Moskal, A. Grabowski, A. Lisiecki, Laser remelting of silicide coatings on Mo and TZM alloy, Solid State Phenomena 226 (2015) 121-126, DOI: https://doi.org/10.4028/www.scientific.net/SSP.226.121.
[5] T. Kik, J. Moravec, I. Novakova, New method of processing heat treatment experiments with numerical simulation support, Proceedings of the Modtech International Conference – Modern Technologies in Industrial Engineering V, Vol. 227, 2017, Article Number: UNSP 012069.
[6] R. Burdzik, T. Węgrzyn, Ł. Konieczny, A. Lisiecki, Research on influence of fatigue metal damage of the inner race of bearing on vibration in different frequencies, Archives of Metallurgy and Materials 59/4 (2014) 1275-1281, DOI: https://doi.org/10.2478/amm-2014-0218.
[7] A. Lisiecki, Welding of titanium alloy by different types of lasers, Archives of Materials Science and Engineering 58/2 (2012) 209-218.
[8] K. Labisz, T. Tański, D. Janicki, W. Borek, K. Lukaszkowicz, L.A. Dobrzański, Effect of laser feeding on heat treated aluminium alloy surface properties, Archives of Metallurgy and Materials 61/2 (2016) 741-746, DOI: https://doi.org/10.1515/amm-2016-0126.
[9] A. Lisiecki, D. Ślizak, A. Kukofka, Robotic fiber laser cladding of steel substrate with iron-based metallic powder, Materials Performance and Characterization 8/6 (2019) 1202-1213, DOI: https://doi.org/10.1520/MPC20190068.
[10] A. Lisiecki, Study of optical properties of surface layers produced by laser surface melting and laser surface nitriding of titanium alloy, Materials 12 (2019) 3112, DOI: https://doi.org/10.3390/ma12193112.
[11] A. Kurc-Lisiecka, A. Lisiecki, Hybrid Laser-GMA Welding of High-Strength Steel Grades, Materials Performance and Characterization 8/4 (2019) 614-625, DOI: https://doi.org/10.1520/MPC20190070.
[12] J. Górka, T. Kik, A. Czupryński, W. Foreiter, Technology of welding hard wearing plates, Welding International 28/10 (2014) 749-755, DOI: https://doi.org/10.1080/09507116.2012.753223.
[13] A. Lisiecki, D. Ślizak, A. Kukofka, Robotized Fiber Laser Cladding of Steel Substrate by Metal Matrix Composite Powder at Cryogenic Conditions, Materials Performance and Characterization 8/6 (2019) 1214-1225, DOI: https://doi.org/10.1520/MPC20190069.
[14] A. Klimpel, A. Czupryński, J. Górka, T. Kik, M. Melcer, A study of modern materials for arc spraying, Welding International 28/2 (2014) 100-106, DOI: https://doi.org/10.1080/09507116.2012.708479.
[15] A. Klimpel, L.A. Dobrzański, A. Lisiecki, D. Janicki, The study of properties of Ni-WC wires surfaced deposits, Journal of Materials Processing Technology 164-165 (2005) 1046-1055, DOI: https://doi.org/10.1016/j.jmatprotec.2005.02.195.
[16] A. Lisiecki, R. Burdzik, P. Folęga, B. Oleksiak, Ł. Konieczny, G. Siwiec, J. Warczek, Disk laser welding of car body zinc coated steel sheets, Archives of Metallurgy and Materials 60/4 (2015) 2913-2922, DOI: https://doi.org/10.1515/amm-2015-0465.
[17] J. Górka, A. Czupryński, M. Żuk, M. Adamiak, A. Kopyść, Properties and structure of deposited nanocrystalline coatings in relation to selected construction materials resistant to abrasive wear, Materials 11/7 (2018) 1184, DOI: https://doi.org/10.3390/ma11071184.
[18] A. Świerczyńska, J. Łabanowski, J. Michalska, D. Fydrych, Corrosion behavior of hydrogen charged super duplex stainless steel welded joints, Materials and Corrosion 68/10 (2017) 1037-1045, DOI: https://doi.org/10.1002/maco.201709418.
[19] A. Lisiecki, Mechanism of laser surface modification of the Ti-6Al-4V alloy in nitrogen atmosphere using a high power diode laser, Advanced Materials Research 1036 (2014) 411-416, DOI: https://doi.org/10.4028/www.scientific.net/AMR.1036.411.
[20] A. Lisiecki, J. Piwnik, Tribological characteristic of titanium alloy surface layers produced by diode laser gas nitriding, Archives of Metallurgy and Materials 61/2 (2016) 543-552, DOI: https://doi.org/10.1515/amm-2016-0094.
[21] A. Kurc-Lisiecka, Impact toughness of laser-welded butt joints of the new steel grade strenx 1100MC, Materiali in Tehnologije 51/4 (2017) 643-649, DOI: https://doi.org/10.17222/ mit.2016.234.
[22] A. Lisiecki, Mechanisms of hardness increase for composite surface layers during laser gas nitriding of the Ti6Al4V alloy, Materiali in Tehnologije 51/4 (2017) 577-583, DOI: https://doi.org/10.17222/mit.2016.106.

[23] A. Lisiecki, A. Kurc-Lisiecka, Erosion wear resistance of titanium-matrix composite Ti/TiN produced by diode-laser gas nitriding, 51/1 (2017) 29-34, DOI: https://doi.org/10.17222/mit.2015.160.

[24] M. Staszuk, L.A. Dobrzański, T. Tański, W. Kwaśny, M. Musztyfaga-Staszuk, The effect of PVD and CVD coating structures on the durability of sintered cutting edges, Archives of Metallurgy and Materials 59/1 (2014) 269-274, DOI: https://doi.org/10.2478/amm-2014-0044.

[25] A. Grajcar, A. Plachcińska, S. Topolska, M. Kciuk, Effect of thermomechanical treatment on the corrosion behaviour of Si- and Al-containing high-Mn austenitic steel with Nb and Ti micro-additions, Materiali in Tehnologije 49/6 (2015) 889-894, DOI: https://doi.org/10.17222/mit.2014.148.

[26] J. Xiong, F. Nie, H. Zhao, L. Zheng, J. Luo, L. Yang, Z. Wen, Microstructure Evolution and Failure Behavior of Stellite 6 Coating on Steel after Long-Time Service, Coatings 9/9 (2019) 532, DOI: https://doi.org/10.3390/coatings9090532.

[27] M.M. Ferozhkhan, M. Duraiselvam, K.G Kumar, R. Ravibharath, Plasma transferred arc welding of Stellite 6 alloy on stainless steel for wear resistance, Procedia Technology 25 (2016) 1305-1311, DOI: https://doi.org/10.1016/j.protcy.2016.08.226.

[28] G.R Mirshekari, S. Daee, S.F. Bonabi, M.R. Tavakoli, A. Shafyei, M. Safaeia, Efect of interlayers on the microstructure and wear resistance of Stellite 6 coatings deposited on AISI 420 stainless steel by GTAW technique, Surfaces and Interfaces 9 (2017) 79-92, DOI: https://doi.org/10.1016/j.surfin.2017.08.005.

[29] F. Molleda, J. Mora, F.J. Molleda, E. Mora, E. Carrillo, B.G. Mellor, A study of the solid–liquid interface in cobalt base alloy (Stellite) coatings deposited by fusion welding (TIG), Materials Characterization 57/4-5 (2006) 227-231, DOI: https://doi.org/10.1016/j.matchar.2006.01.016.

[30] T. Giętka, K. Ciechacki, T. Kik, Numerical Simulation of Duplex Steel Multipass Welding, Archives of Metallurgy and Materials 61 (2016) 1975-1984, DOI: https://doi.org/10.1515/amm-2016-0319.

[31] T. Kik, J. Moravec, I. Novakova, Application of Numerical Simulations on 10GN2MFA Steel Multilayer Welding, Dynamical Systems in Applications 249 (2018) 193-204, DOI: https://doi.org/10.1007/978-3-319-96601-4_18.

[32] A. Kurc-Lisiecka, A. Lisiecki, Weld metal toughness of autogenous laser-welded joints of high-strength steel DOMEX 960, Materials Performance and Characterization 8/6 (2019) 1226-1236, DOI: https://doi.org/10.1520/MPC20190071.

[33] J. Moravec, I. Novakova, J. Sobotka, T. Kik, Application possibilities of the low-temperature repairs on creep-resistance turbine components from material GX23CrMoV12-1, Innovative Technologies in Engineering Production (ITEP'18) Book Series: MATEC Web of Conferences, Vol. 244, 2018, 01017.

[34] J. Moravec, T. Kik, I. Novakova, Application of numerical simulations on X10CrWMoVNb9-2 steel multilayer welding, MM Science Journal (2016) 1190-1193, DOI: https://doi.org/10.17973/MMSJ.2016_11_201628.

[35] Z .Wang, J. Zhao, Y. Zhao, H. Zhang, F. Shi, Microstructure and Microhardness of Laser Metal Deposition Shaping K465/Stellite-6 Laminated Material, Metals 7 (2017) 512, DOI: https://doi.org/ 10.3390/met7110512.

[36] A. Razavykia, C. Delprete, P. Baldissera, Correlation between Microstructural Alteration, Mechanical Properties and Manufacturability after Cryogenic Treatment: A Review, Materials 12/20 (2019) 3302, DOI: https://doi.org/10.3390/ma12203302.

[37] A. Zieliński, M. Jażdżewska, A. Narożniak-Łuksza, W. Serbiński, Surface structure and properties of Ti6Al4V alloy laser melted at cryogenic conditions, Journal of Achievements in Materials and Manufacturing Engineering 18 (2006) 423-426.

[38] A. Zieliński, W. Serbiński, B. Majkowska, M. Jażdżewska, I. Skalski, Influence of laser remelting st cryogenic conditions on corrosion resistance of non-ferrous alloys, Advances in Materials Science 9/4 (2009) 21-28, DOI: https://doi.org/10.2478/v10077-009-0018-9.

[39] B. Majkowska, W. Serbiński, Cavitation wearing of the SUPERSTON alloy after laser treatment at cryogenic conditions, Solid State Phenomena 165 (2010) 306-309, DOI: https://doi.org/10.4028/www.scientific.net/SSP.165.306.